ChemComm

Biocompatible photoinduced CuAAC using sodium pyruvate

Journal:	*ChemComm*
Manuscript ID	CC-COM-10-2021-005566.R1
Article Type:	Communication

COMMUNICATION

Biocompatible photoinduced CuAAC using sodium pyruvate†

Jaepil Jeong[a], Grzegorz Szczepaniak,*[ab] Saigopalakrishna S. Yerneni,[c] Francesca Lorandi,[a] Hossein Jafari,[a] Sushil Lathwal,[a] Subha R. Das,*[ad] and Krzysztof Matyjaszewski1*[a]

Received 00th January 20xx,
Accepted 00th January 20xx

DOI: 10.1039/x0xx00000x

Sodium pyruvate, a natural intermediate produced during cellular metabolism, is commonly used in buffer solutions and media for biochemical applications. Here we show the use of sodium pyruvate (SP) as a reducing agent in a biocompatible aqueous photoinduced azide-alkyne cycloaddition (CuAAC) reaction. This copper(I)-catalyzed 1,3-dipolar cycloaddition is triggered by SP under UV light irradiation, exhibits oxygen tolerance and temporal control, and provides a convenient alternative to current CuAAC systems, particularly for biomolecular conjugations.

The copper(I)-catalyzed azide-alkyne cycloaddition (CuAAC), introduced in 2001 by Sharpless and co-workers, is the most recognized click reaction.[1] This transformation enables the rapid, efficient, and regioselective formation of 1,4-disubstituted 1,2,3-triazoles under mild conditions. As a result, CuAAC has found broad application in multiple fields as a tool for covalent linkage of a wide variety of materials,[2, 3] including nanoparticles,[4] polymers,[5, 6] DNA,[7] RNA,[8-11] carbohydrates,[12] proteins,[13] and cells.[14, 15] Although Cu(I) species can be used directly as catalysts,[16] the *in situ* reduction of air-stable Cu(II) precatalysts considerably simplifies the reaction setup. Sodium ascorbate is the most commonly used reducing agent in CuAAC reactions.[1, 17] Alternatively, Cu^{II}/L complexes (L = ligand) can be directly reduced when excess ligand is used under light irradiation or in the presence of a photocatalyst or radical photoinitiator.[18-41] The photoinduced approach offers spatial and temporal control over the reaction.[18, 19] However, many radical photoinitiators (e.g., phenylbis(acyl) phosphine oxide and diphenyl(acyl) phosphine oxide) and their photolysis products can cause cytotoxicity.[42, 43] Furthermore, the poor solubility of some widely used photocatalysts and photoinitiators in water also limits their biological applications.

Sodium pyruvate (**SP**) is a cellular metabolic intermediate,[44] that is commonly used in cell culture media, where it serves as a carbon and energy source in addition to glucose.[45] **SP** is highly soluble in water (100 mg/mL) and can scavenge reactive oxygen species (e.g., hydrogen peroxide).[46, 47]

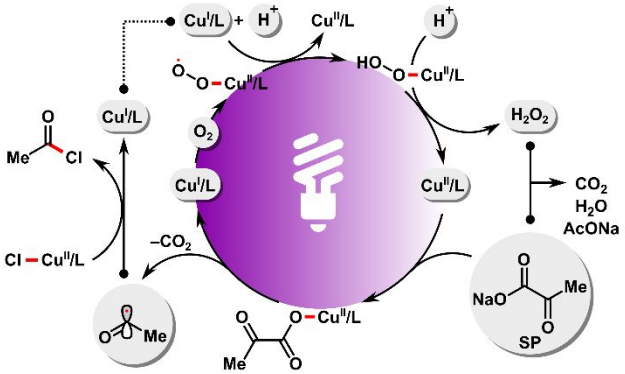

Fig. 1 Proposed mechanism of Cu^{II}/L reduction by **SP** under UV light irradiation in an ambient atmosphere.

Inspired by the recent use of **SP** in Cu-catalyzed atom transfer radical polymerization (ATRP),[48] here we demonstrate an oxygen-tolerant, photoinduced CuAAC triggered by **SP** under biologically relevant conditions. In the proposed system, **SP** participates in an association/dissociation equilibrium with a Cu^{II}/L complex (Fig. 1). Under UV light irradiation, the carbon-carbon bond in the copper-pyruvate complex undergoes homolytic cleavage and decomposes into an acyl radical, carbon dioxide, and the corresponding Cu^{I}/L catalyst. The acyl radical can then reduce another molecule of Cu^{II}/L to Cu^{I}/L, forming acyl chloride (Fig. 1). This secondary process increases the rate of copper reduction. Since the oxidized catalyst is continuously converted back to its active reduced form, the catalytic system acts as an oxygen scavenger, providing oxygen tolerance. The addition of a buffer to the reaction mixture prevents pH

[a] *Department of Chemistry, Carnegie Mellon University, Pittsburgh, Pennsylvania 15213, United States. Email: gszczepa@andrew.cmu.edu, srdas@andrew.cmu.edu, matyjaszewski@cmu.edu*
[b] *University of Warsaw, Faculty of Chemistry, Pasteura 1, 02-093 Warsaw, Poland*
[c] *Department of Biomedical Engineering, Carnegie Mellon University, Pittsburgh, Pennsylvania 15213, United States.*
[d] *Center for Nucleic Acids Science & Technology, Carnegie Mellon University, Pittsburgh, Pennsylvania 15213, United States.*
†Electronic Supplementary Information (ESI) available. See DOI: 10.1039/x0xx00000x

changes caused by the hydrolysis of the acyl chloride. The SP-based CuAAC described here is a practical and convenient tool in modifying expensive or hard-to-synthesize biomolecules at low volumes under ambient conditions.

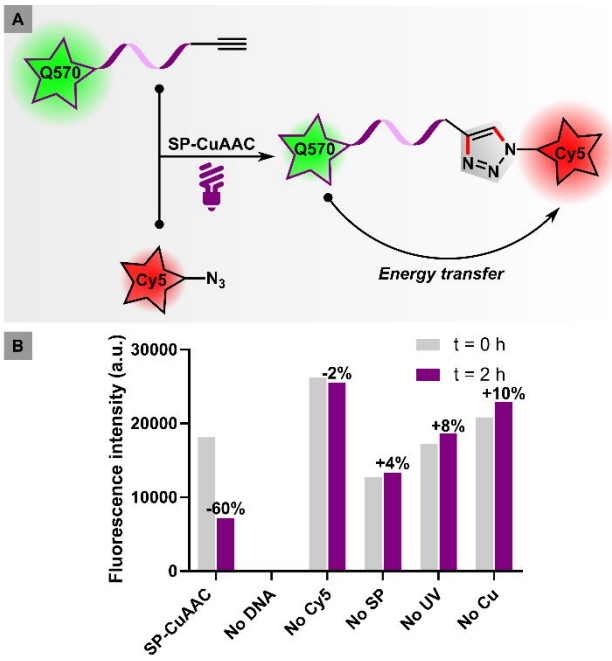

Fig. 2 SP-mediated photoinduced CuAAC, reaction conditions: [Q570-DNA]/[N_3-Cy5]/[$CuSO_4$]/[THPTA]/[SP]: 1/1.1/2.5/12.5/1000, [Q570-DNA] = 0.1 mM, in PBS with 3.7 % DMSO at r.t., under UV light (6 mW/cm^2) in an ambient atmosphere for 2 h. (A) Förster resonance energy transfer occurs upon SP-CuAAC. (B) Microplate reader measurement of the Q570 fluorescence intensity drop (λ_{ex} = 548 nm, λ_{em} = 568 nm) due to FRET.

To examine the SP-CuAAC reaction in biomolecular conjugations, a set of experiments was performed to evaluate the influence of the individual reagents (Fig. 2). A 10-mer DNA T10 strand functionalized with 3'-terminal Quasar 570 (Q570) dye and 5'-hexynyl functional group was used as a model compound (Fig. 2A). The CuAAC reaction between the Q570-DNA alkyne (Q570-DNA, 0.1 mM) and azide-modified Cyanine 5 dye (N3-Cy5, 0.11 mM) was conducted by mixing $CuSO_4$ (0.25 mM), tris-hydroxypropyltriazolylmethylamine (THPTA, 1.25 mM) and **SP** (100 mM) in phosphate-buffered saline (PBS) solution with DMSO (3.7% v/v). The reactions were carried out under UV irradiation (365 nm, 2 or 6 mW/cm^2) in an ambient atmosphere at a reaction volume of 100 µL and analyzed by fluorescence and HPLC methods.

After the click Cy5 conjugation, the short distance between the Q570 and Cy5 dyes attached to the DNA causes Förster resonance energy (FRET) transfer: the fluorescence of Q570 decreases (Fig 2A), while the fluorescence of Cy5 increases (ESI Fig. S1). This allows to determine the conversion of the conjugation by measuring the intensity drop in the Q570 fluorescence. In the absence of any of the components (substrates, **SP**, UV irradiation, or $CuSO_4$), no energy transfer from Q570 to Cy5 was observed, confirming that all reagents are necessary to form the desired conjugate (Fig. 2B). Importantly, we found that the Q570 dye is very stable under UV light irradiation (6 mW/cm^2), indicating that the decrease in its fluorescence after CuAAC reactions was not caused by photobleaching (ESI Fig. S2).[49]

Next, we searched for optimal conditions for the SP-CuAAC (ESI Fig S3). The optimal loading of $CuSO_4$ was determined to be 2.5 equivalents relative to the DNA alkyne, which is similar to benchmark aqueous CuAAC conditions.[17] Interestingly, the conjugation conversion decreased at higher copper concentrations, as we have observed previously for CuAAC conjugations.[9] A possible explanation is that, during the photoreduction, the high Cu^{II}/L loading leads to increased generation of hydroperoxyl radicals that act as strong oxidants.[50, 51]

The effect of light intensity and wavelength on the reaction process was investigated (ESI Fig. S4 and S5). When a lower intensity UV lamp (365 nm, 2 mW/cm^2) was used (ESI Fig. S4C), the Cu^{II}/L photoreduction was slower. Although the reaction time increased to 150 min, the final conjugation conversion was comparable with the result obtained using higher intensity irradiation (365 nm, 6 mW/cm^2), implying that it is possible to accelerate and decelerate the reaction on demand by simply changing the light source. Importantly, no conjugation was observed under either green (520 nm, 8 mW/cm^2) or white light (400–700 nm, 6 mW/cm^2) irradiation (ESI Fig. S5), indicating that UV light is essential for triggering SP-CuAAC reaction.

The reaction mixtures were also analyzed by HPLC (ESI Fig. S4). As the reaction proceeded, the characteristic absorption peak of the DNA-alkyne substrate decreased (elution time: approx. 11 min), and a new peak from the conjugate increased (elution time: approx. 13 min). The reaction reached 90% substrate conversion after 45 minutes of UV irradiation (6 mW/cm^2) (ESI Fig. S4A). The HPLC conversion from Fig. S4A was compared to the fluorescence factor (F/F0, where F and F0 are the fluorescence intensity of Q570 after and before the reaction). We verified that the HPLC conversion can be approximated by a linear function of F/F0 (ESI Fig. S6A). Fig. S6B shows that the conversions calculated from the fitted linear function and the conversions measured by HPLC from Fig. S4 were in good agreement, especially for conversions higher than 30%.

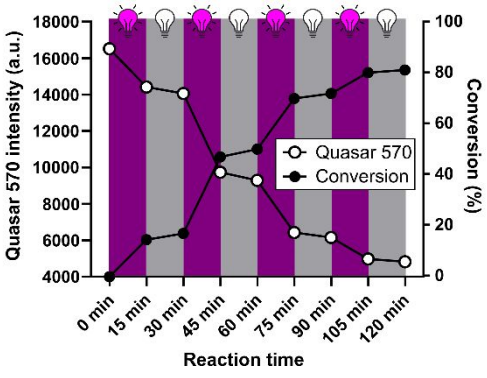

Fig. 3 Temporal control in SP-CuAAC, reaction conditions: [Q570-DNA]/[N_3-Cy5]/[$CuSO_4$]/[THPTA]/[SP]: 1/1.1/2.5/12.5/1000, [Q570-DNA] = 0.1 mM, in PBS with 3.7 % DMSO at r.t., under UV light (6 mW/cm^2) in an ambient atmosphere. The conversion was calculated using the F/F0 of Q570 and the linear regression equation from Fig. S6A.

Temporal control of the SP-CuAAC was demonstrated by turning the UV light on and off. As shown in Fig. 3, the fluorescence decrease of the Q570 dye (white circle) was observed when the UV light was turned on. During each irradiation period, an average of 20% conversion increase was achieved. This average value was slightly lower than with continuous irradiation for a similar time interval, and the final conversion (81%) was also slightly lower. This may be attributed to the diffusion of oxygen into the solution during the light-off periods. A similar result was observed when UV light on and off time was increased to 30 min (Fig. S7). Additionally, the CuAAC reaction did not stop immediately after turning off the light due to residual Cu^{I}/L present in the solution.[52, 53] Nonetheless, this result shows that the **SP** can mediate the rapid photoreduction of Cu^{II}/L in a time-controlled manner, even without deoxygenation of the reaction mixture.

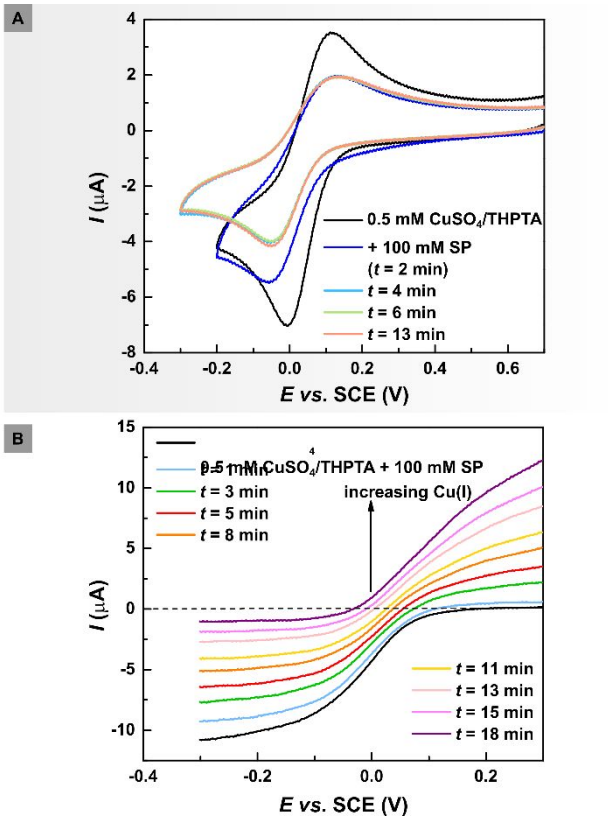

Fig. 4 (A) CVs of 0.5 mM $Cu^{II}SO_4$/THPTA in PBS, recorded on a glassy carbon (GC) working electrode at v = 0.2 Vs^{-1}, in the absence and presence of 100 mM **SP**. (B) LSV of 0.5 mM Cu^{II}/THPTA + 100 mM **SP**, in PBS, recorded on a GC working electrode at v = 0.01 Vs^{-1} under UV light (3.6 mW/cm^2). The GC tip was attached to a rotating disk electrode (RDE), rotating at a speed of 2500 rpm.

To evaluate the proposed Cu^{II}/L photoreduction mechanism SP-CuAAC (Fig. 1), we investigated the reactivity of **SP** toward the Cu^{II}/THPTA complex (Fig. 4A). Cyclic voltammetry (CV) showed that upon the addition of 100 mM **SP** to the Cu^{II}/THPTA complex in PBS, the peak corresponding to the reduction of the Cu(II) complex shifted to more negative values (ca. 20 mV) and decreased in intensity. The relative oxidation peak potential remained constant, but its intensity decreased as well. This indicated that the pyruvate anion interacted with the $Cu^{II}SO_4$/THPTA complex, presumable forming the $(CH_3C(O)CO_2)$–Cu^{II}/THPTA complex with slightly more negative reduction potential than $Cu^{II}SO_4$/THPTA and reversible electrochemical behavior. Next, the generation of Cu^{I}/L catalyst was investigated by electrochemical analysis (Fig. 4B).[54] The $(CH_3C(O)CO_2)$–Cu^{II}/THPTA complex was irradiated by UV light in a deoxygenated environment and monitored by linear sweep voltammetry (LSV). We obtained the rate constant of reduction k_{red} = 1.9 x 10^{-3} s^{-1} (Fig. S8), confirming that photoreduction indeed occurs. This constant is likely to be affected by the presence of oxygen and light intensity.

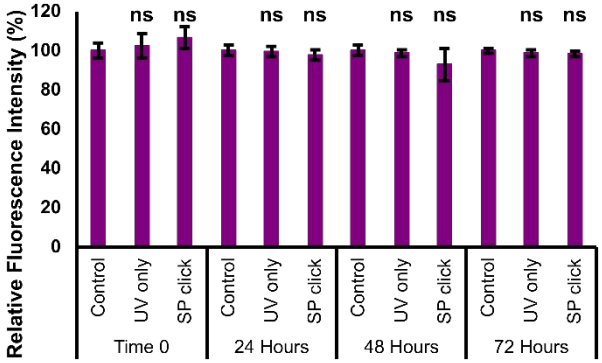

Fig. 5 Cytotoxicity and proliferation assay. HEK293 cells were subjected to SP-CuAAC reaction for 30 min at 4 °C followed by a proliferation assay over a period of 72 hours. Bars indicate mean ± SEM (n=3), ns: no significant difference vs. control group (no treatment).

To further evaluate the biocompatibility of this method, we attempted SP-based CuAAC reaction in the presence of human embryonic kidney 293 (HEK293) cells in a 96-well plate (Fig. 5). Cytotoxicity and proliferation assay showed that the SP-CuAAC conditions did not cause significant damage to HEK293 cells after the irradiation with strong UV light (6 mW/cm^2) for 30 min. However, a conversion of 47% was obtained, which was ~13% lower than in the model system (Fig. S9). In our hypothesis, the discrepancy of conversion in the culture condition is due to the continuous diffusion of oxygen from the atmosphere into the culture plate.

In conclusion, we have developed a new photoinduced CuAAC system based on highly water-soluble sodium pyruvate as a non-toxic photo-reducing agent. Sodium pyruvate continuously reduces the oxidized copper catalyst under UV light irradiation, allowing the *in situ* chemical removal of oxygen and maintaining CuAAC reaction under an ambient atmosphere. Non-experts can easily apply this straightforward method to conjugate functional materials onto DNA, proteins, and cells at low volumes in a temporally controlled manner under physiological conditions.

This work was supported by NSF (CHE-2000391). GS gratefully acknowledges the Polish Ministry of Science and Higher Education ("Mobilnosc Plus" grant no. 1646/MOB/V/2017/0) for financial support.

Conflicts of interest

There are no conflicts to declare.

References

1. V. V. Rostovtsev, L. G. Green, V. V. Fokin and K. B. Sharpless, *Angew. Chem. Int. Ed.*, 2002, **41**, 2596-2599.
2. P. Thirumurugan, D. Matosiuk and K. Jozwiak, *Chem. Rev.*, 2013, **113**, 4905-4979.
3. W. Xi, T. F. Scott, C. J. Kloxin and C. N. Bowman, *Adv. Funct. Mater.*, 2014, **24**, 2572-2590.
4. N. Li and W. H. Binder, *J. Mater. Chem.*, 2011, **21**, 16717-16734.
5. J.-F. Lutz, *Angew. Chem. Int. Ed.*, 2007, **46**, 1018-1025.
6. P. L. Golas and K. Matyjaszewski, *QSAR & Combinatorial Science*, 2007, **26**, 1116-1134.
7. A. H. El-Sagheer and T. Brown, *Chem. Soc. Rev.*, 2010, **39**, 1388-1405.
8. C. Y. Jao and A. Salic, *Proc. Natl. Acad. Sci. U. S. A.*, 2008, **105**, 15779.
9. E. Paredes and S. R. Das, *ChemBioChem*, 2011, **12**, 125-131.
10. E. Paredes and S. R. Das, *Bioorg. Med. Chem. Lett.*, 2012, **22**, 5313-5316.
11. S. E. Averick, E. Paredes, S. K. Dey, K. M. Snyder, N. Tapinos, K. Matyjaszewski and S. R. Das, *J. Am. Chem. Soc.*, 2013, **135**, 12508-12511.
12. A. K. Agrahari, P. Bose, M. K. Jaiswal, S. Rajkhowa, A. S. Singh, S. Hotha, N. Mishra and V. K. Tiwari, *Chem. Rev.*, 2021, **121**, 7638-7956.
13. A. E. Speers and B. F. Cravatt, *Chem. Biol.*, 2004, **11**, 535-546.
14. V. Hong, N. F. Steinmetz, M. Manchester and M. G. Finn, *Bioconjugate Chem.*, 2010, **21**, 1912-1916.
15. Y.-Y. Guo, B. Zhang, L. Wang, S. Huang, S. Wang, Y. You, G. Zhu, A. Zhu, M. Geng and L. Li, *Chem. Commun.*, 2020, **56**, 14401-14403.
16. T. R. Chan, R. Hilgraf, K. B. Sharpless and V. V. Fokin, *Org. Lett.*, 2004, **6**, 2853-2855.
17. V. Hong, S. I. Presolski, C. Ma and M. G. Finn, *Angew. Chem. Int. Ed.*, 2009, **48**, 9879-9883.
18. G. S. Kumar and Q. Lin, *Chem. Rev.*, 2021, **121**, 6991-7031.
19. B. D. Fairbanks, L. J. Macdougall, S. Mavila, J. Sinha, B. E. Kirkpatrick, K. S. Anseth and C. N. Bowman, *Chem. Rev.*, 2021, **121**, 6915-6990.
20. C. Kütahya, Y. Zhai, S. Li, S. Liu, J. Li, V. Strehmel, Z. Chen and B. Strehmel, *Angew. Chem. Int. Ed.*, 2021, **60**, 10983-10991.
21. R. Martínez-Haya, A. A. Heredia, W. D. Castro-Godoy, L. C. Schmidt, M. L. Marin and J. E. Argüello, *J. Org. Chem.*, 2021, **86**, 5832-5844.
22. Y. You, F. Cao, Y. Zhao, Q. Deng, Y. Sang, Y. Li, K. Dong, J. Ren and X. Qu, *ACS Nano*, 2020, **14**, 4178-4187.
23. A. U. Shete, B. P. Sutherland and C. J. Kloxin, *Polym. Chem.*, 2020, **11**, 7515-7523.
24. C. Kütahya, Y. Yagci and B. Strehmel, *ChemPhotoChem*, 2019, **3**, 1180-1186.
25. O. Jennah, R. Beniazza, C. Lozach, D. Jardel, F. Molton, C. Duboc, T. Buffeteau, A. El Kadib, D. Lastécouères, M. Lahcini and J.-M. Vincent, *Adv. Synth. Catal.*, 2018, **360**, 4615-4624.
26. O. S. Taskin, G. Yilmaz and Y. Yagci, *ACS Macro Lett.*, 2016, **5**, 103-107.
27. O. Yetiskin, S. Dadashi-Silab, S. B. Khan, A. M. Asiri and Y. Yagci, *Asian J. Org. Chem.*, 2015, **4**, 442-444.
28. O. S. Taskin, S. Dadashi-Silab, B. Kiskan, J. Weber and Y. Yagci, *Macromol. Chem. Phys.*, 2015, **216**, 1746-1753.
29. S. Dadashi-Silab and Y. Yagci, *Tetrahedron Lett.*, 2015, **56**, 6440-6443.
30. M. Arslan, G. Yilmaz and Y. Yagci, *Polym. Chem.*, 2015, **6**, 8168-8175.
31. G. Yilmaz, B. Iskin and Y. Yagci, *Macromol. Chem. Phys.*, 2014, **215**, 662-668.
32. Y. Yagci, M. A. Tasdelen and S. Jockusch, *Polymer*, 2014, **55**, 3468-3474.
33. S. Dadashi-Silab, B. Kiskan, M. Antonietti and Y. Yagci, *RSC Adv.*, 2014, **4**, 52170-52173.
34. J. C. Bear, N. Hollingsworth, P. D. McNaughter, A. G. Mayes, M. B. Ward, T. Nann, G. Hogarth and I. P. Parkin, *Angew. Chem. Int. Ed.*, 2014, **53**, 1598-1601.
35. A. A. Alzahrani, A. H. Erbse and C. N. Bowman, *Polym. Chem.*, 2014, **5**, 1874-1882.
36. T. Gong, B. J. Adzima and C. N. Bowman, *Chem. Commun.*, 2013, **49**, 7950-7952.
37. M. A. Tasdelen, G. Yilmaz, B. Iskin and Y. Yagci, *Macromolecules*, 2012, **45**, 56-61.
38. L. Harmand, S. Cadet, B. Kauffmann, L. Scarpantonio, P. Batat, G. Jonusauskas, N. D. McClenaghan, D. Lastécouères and J.-M. Vincent, *Angew. Chem. Int. Ed.*, 2012, **51**, 7137-7141.
39. B. J. Adzima, Y. Tao, C. J. Kloxin, C. A. DeForest, K. S. Anseth and C. N. Bowman, *Nat. Chem.*, 2011, **3**, 256-259.
40. M. A. Tasdelen and Y. Yagci, *Tetrahedron Lett.*, 2010, **51**, 6945-6947.
41. S. C. Ritter and B. König, *Chem. Commun.*, 2006, 4694-4696.
42. C. G. Williams, A. N. Malik, T. K. Kim, P. N. Manson and J. H. Elisseeff, *Biomaterials*, 2005, **26**, 1211-1218.
43. M. Popal, J. Volk, G. Leyhausen and W. Geurtsen, *Dent. Mater.*, 2018, **34**, 1783-1796.
44. Y. Wang, Y. Huang, J. Yang, F.-Q. Zhou, L. Zhao and H. Zhou, *Military Med Res*, 2018, **5**, 13.
45. J. C. Willison, *Microbiology*, 1988, **134**, 2429-2439.
46. A. R. Giandomenico, G. E. Cerniglia, J. E. Biaglow, C. W. Stevens and C. J. Koch, *Free Radical Biol. Med.*, 1997, **23**, 426-434.
47. A. Lopalco, G. Dalwadi, S. Niu, R. L. Schowen, J. Douglas and V. J. Stella, *J. Pharm. Sci.*, 2016, **105**, 705-713.
48. G. Szczepaniak, M. Łagodzińska, S. Dadashi-Silab, A. Gorczyński and K. Matyjaszewski, *Chem. Sci.*, 2020, **11**, 8809-8816.
49. J. Widengren and R. Rigler, *Bioimaging*, 1996, **4**, 149-157.
50. E. Lallana, R. Riguera and E. Fernandez-Megia, *Angew. Chem. Int. Ed.*, 2011, **50**, 8794-8804.
51. A. Kumar, K. Li and C. Cai, *Chem. Commun.*, 2011, **47**, 3186-3188.
52. S. Dadashi-Silab, I.-H. Lee, A. Anastasaki, F. Lorandi, B. Narupai, N. D. Dolinski, M. L. Allegrezza, M. Fantin, D. Konkolewicz, C. J. Hawker and K. Matyjaszewski, *Macromolecules*, 2020, **53**, 5280-5288.
53. X. Pan, M. Fantin, F. Yuan and K. Matyjaszewski, *Chem. Soc. Rev.*, 2018, **47**, 5457-5490.
54. S. Dadashi-Silab, F. Lorandi, M. J. DiTucci, M. Sun, G. Szczepaniak, T. Liu and K. Matyjaszewski, *J. Am. Chem. Soc.*, 2021, **143**, 9630-9638.